optics

MDPI

Article

Non-Destructive Identification of Drugs in Plastic Packaging Using Attenuated Total Reflection Terahertz Time Domain Spectroscopy

Kazuma Hashimoto [1] and Saroj R. Tripathi [1,2,*]

[1] Department of Mechanical Engineering, Shizuoka University, 3-5-1 Johoku, Hamamatsu 432-8013, Japan; hashimoto.kazuma.17@shizuoka.ac.jp
[2] Graduate School of Science and Technology, Shizuoka University, 3-5-1 Johoku, Hamamatsu 432-8013, Japan
* Correspondence: sarojrt@outlook.com

Abstract: In this study, we demonstrate that drugs in plastic packaging can be identified without being opened using attenuated total reflection terahertz time domain spectroscopy. In this system, the terahertz wave undergoes total internal reflection at the interface between prism and sample, producing an evanescent wave at the interface. The penetration depth of the evanescent waves is larger than the thickness of typical plastic packaging in the sub-terahertz frequency region; therefore, it becomes possible to detect the sample without opening the package. Here, we show that some saccharides samples such as lactose in plastic packaging can be identified using its spectral fingerprint by placing the packaged lactose on the prism. This method has the potential to be used in the non-destructive testing and analysis of a wide variety of samples, such as medicine sachets, to reduce medication dispensing errors in pharmacies.

Keywords: terahertz; spectroscopy; non-destructive testing; attenuated total reflection; refractive index; absorption coefficient

check for updates

Citation: Hashimoto, K.; Tripathi, S.R. Non-Destructive Identification of Drugs in Plastic Packaging Using Attenuated Total Reflection Terahertz Time Domain Spectroscopy. *Optics* **2022**, 3, 99–106. https://doi.org/10.3390/opt3020012

Academic Editor: Thomas Seeger

Received: 27 February 2022
Accepted: 18 March 2022
Published: 22 March 2022

1. Introduction

Terahertz waves lie in between the microwave and infrared regions in the electromagnetic spectrum. These waves have enormous potential in various applications such as biomedicine, information, and communication technology, homeland security, pharmaceutical science and many more [1]. Besides these applications, terahertz waves are also being explored in non-destructive testing and analysis applications because of their unique characteristics, such as high sensitivity to water and the ability to penetrate through a wide variety of nonmetallic materials such as plastics, papers, fabrics, ceramics, and various construction materials [2]. One of the well-known applications of THz waves is the non-destructive sensing and imaging of illicit drugs and explosives based upon their spectral fingerprints [3–5].

The vast majority of terahertz wave measurements have been conducted using terahertz time domain spectroscopy (THz-TDS). It is a method used to determine the frequency dependent optical constants such as refractive index and absorption coefficients of material by probing with a subpicosecond pulse of the THz wave [6]. THz-TDS in transmission mode involves the recording of time-domain pulses of the THz electric field transmitted through the sample under investigation and a reference signal in the absence of the sample. These signals are transformed to the frequency domain using a fast Fourier transformation to compute their intensity and phase spectra. Finally, these spectra, along with the thickness of the sample, are used to determine frequency dependent THz properties such as the refractive index and the absorption coefficient of the sample [7,8]. The transmission mode THz-TDS system has been used in various non-destructive testing and evaluation applications. For example, THz waves have been used to detect foreign bodies in various food products, such as chocolate and milk powder [9,10]. Similarly, various construction materials, such as wood and concrete, have also been investigated using transmission mode THz-TDS [11,12]. However, it is often difficult to measure highly absorbing and thick samples in transmission mode THz-TDS as the intensity of the transmitted THz signal decreases exponentially, as given by the Beer-Lambert Law $I = I_0 \exp(-\alpha d)$ where I and I_0 are the transmitted and incident intensity of the THz wave, d is the sample thickness and α is the absorption coefficient of the sample [13]. Therefore, such samples can be measured by reducing the thickness in such a way that the transmitted signal can be measured with a sufficiently high signal to noise ratio [14,15]. The other option would be to use the reflection mode terahertz measurement system, where the reflected signal from the sample is compared with the reflected signal from the metallic mirror (Reflectance $\approx$ 100%) to compute the optical constants. In this process, the relative position of the sample surface with respect to that of the reference mirror strongly affects the relative phase measured; therefore, it is difficult to obtain the accurate optical properties of the sample [16]. In order to overcome such problems, attenuated total reflection terahertz time domain spectroscopy (ATR THz-TDS) can be used. In this method, a sample under investigation is placed on a prism where the THz wave undergoes total internal reflection and the evanescent wave generated at the interface between the prism and sample enables the obtainment of the THz properties of the sample [17–19]. There are several advantages of the ATR THz-TDS system over other THz TDS systems, such as its ability to measure thick and highly absorbing sample [20,21]. Moreover, samples in solid and powdered form can also be measured without a special need for sample preparation. Therefore, the ATR THz-TDS system has a large potential in sensing and imaging applications [22,23].

Despite such advantages of the ATR THz-TDS system, non-destructive testing applications of THz waves are limited to transmission and reflection mode measurement systems. In this article, we present a method to identify a sample packaged in a plastic bag without opening it, using ATR THz-TDS. In the sub-terahertz frequency range, the penetration depth of the evanescent wave is in the range of a few tens of micrometers, which is much larger than the thickness of a typical plastic package. This allows us to obtain the absorption features of the sample without the need of opening the plastic packaging. Here, we used lactose as a test sample, which is known to have absorption peaks in the terahertz frequency region. We identified the lactose sample in a plastic package based upon its spectral fingerprint at 0.53 THz with attenuated total reflection THz-TDS [24]. Since medication dispensing errors are one of the most serious issues in pharmacy [25,26], this method can be used in the non-destructive identification of the medicine in the package.

2. Materials and Methods

2.1. Experiment

Figure 1 shows the terahertz time domain spectroscopy used in our experiment. A femtosecond laser (IMRA Inc., Boston, MA, USA, λ = 780 nm, pulse width < 100 fs, average power = 20 mW, repetition rate = 50 MHz) beam is divided into two equal halves using a beam splitter. The first half of the beam is used to pump the photoconductive antenna for the THz wave emission, whereas the second half is used to excite another photoconductive antenna for the THz wave detection. The emitted THz wave is collimated by an off-axis parabolic mirror and focused on the Silicon prism as shown in Figure 1b. The THz wave is total internally reflected at the interface between the air and sample, which is then guided to the other photoconductive antenna by a pair of off-axis parabolic mirrors. The optical delay stage is used to scan the time domain profile of the THz pulse. This system covers a frequency range of 100 GHz to 3 THz and the maximum dynamic range of the system is about 65 dB at around 200 GHz. This system has a frequency resolution of 24 GHz.

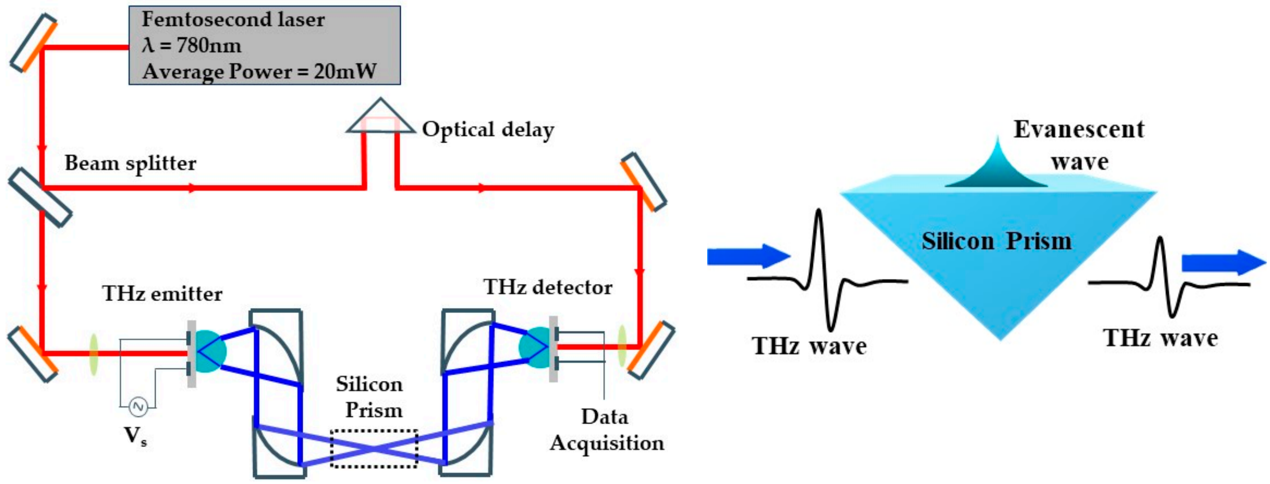

(**a**) (**b**)

Figure 1. (**a**) Schematic diagram of the THz time domain spectrometer. The dotted line shows the position of the Silicon prism in the spectrometer. (**b**) Schematic diagram of a Silicon prism.

In ATR THz-TDS, it is important to note that the refractive index of a prism should be larger than the sample under measurement. We used a high resistivity, low terahertz absorption loss Silicon (Si) prism with a refractive index of 3.41 [27]. When the THz wave undergoes the total internal reflection at the boundary between Si prism surface and air, the total internal reflection creates an evanescent wave that penetrates the sample placed in contact with the prism. The depth of the penetration of evanescent wave is defined as the distance into the sample from the prism-sample interface where the power of the wave is decayed to 1/e of its original value. Mathematically, the depth of the penetration of the evanescent electric field is written using the following equation [28].

$$d_p = \frac{\lambda}{2\pi\sqrt{\left({n_1}^2 \sin^2\theta_i - {n_2}^2\right)}} \tag{1}$$

where λ is the wavelength of the THz wave, n_1 is the refractive index of Silicon prism, n_2 is the refractive index of the sample, and θ_i is the angle of incidence of the incoming THz wave. From Equation (1), it is clear that the depth of penetration mainly depends upon the frequency of the THz wave and the refractive index of the sample, assuming the incident angle (θ_i) and the refractive index of Silicon (n_1) are constant. Therefore, we investigated the penetration depth at a different frequency and refractive index of the sample. Figure 2 shows the dependency of the penetration depth on the sample refractive index (n_2) and frequency. This shows that the depth of penetration increases with the decrease in frequency. Similarly, it also increases with the increase in the refractive index of the sample, as long as the condition $n_1 > n_2$ remains satisfied. This indicates that the THz properties of the sample can be measured even though the sample is packaged in a plastic bag, provided that the bag thickness is less than the penetration depth of the evanescent wave.

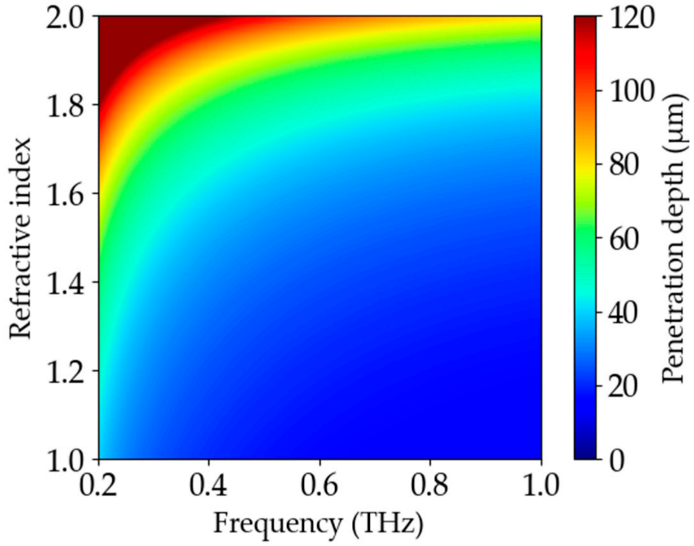

Figure 2. The penetration depth dependency on the frequency of THz wave and the refractive index of the sample. Here, a Silicon prism (n = 3.41) is used as a medium for total internal reflection.

2.2. Sample Preparation

In this study, we used α-lactose monohydrate (Manufacturer: Wako Pure Chemical Industries, purity > 99%) as a test sample since it has absorption features at 0.53 THz, 1.19 THz, and 1.39 THz [24,29]. The particle size of the sample is less than 100 μm. Polyethylene plastic bags are widely used to pack a wide variety of materials such as foods, medicines, dairy products, and so on. The thickness of the polyethylene bags used to pack such materials is in the range of several micrometers. It has a low refractive index and absorption coefficient [30]. In this case, the lactose powder was packaged in a polyethylene plastic bag with a thickness of 10 μm $\pm$ 3 μm, as shown in Figure 3a. The size of the package was approximately 22 mm $\times$ 20 mm. The sample was placed on a Silicon prism, as shown in Figure 3b, to obtain its spectroscopic information.

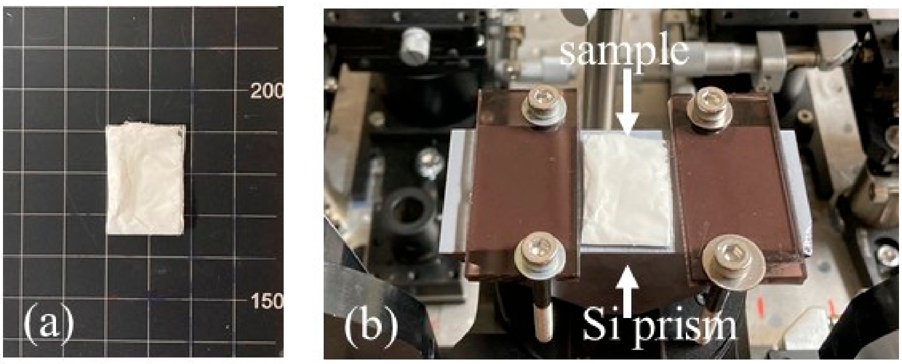

Figure 3. (**a**) Lactose sample packaged in a plastic bag (**b**) Sample placed on the Silicon prism.

3. Results

In our experiment, we first measured the attenuated total reflection, refractive index, and absorption coefficient of a lactose powder. Figure 4a shows the time domain THz pulse with and without placing the sample on a Silicon prism. We repeated the measurement five times and averaged them to increase the signal to noise ratio. Each measurement took approximately 30 s. The THz pulse measured with a sample on a prism is known as the sample pulse $E_{Sam}(t)$, whereas the other pulse is known as the reference pulse $E_{Ref}(t)$. These time domain pulses were transformed to intensity spectra using Fourier transformation, which are written as $E_{Sam}(\omega) = |E_{Sam}(\omega)|\exp\{i\varphi_{Sam}(\omega)\}$ and $E_{Ref}(\omega) =$

$|E_{Ref}(\omega)|\exp\{i\varphi_{Ref}(\omega)\}$; here, $\varphi_{Sam}(\omega)$ and $\varphi_{Ref}(\omega)$ are phase spectra of the sample and reference signals, respectively. Figure 4b shows the intensity spectra of the sample and reference signals, respectively.

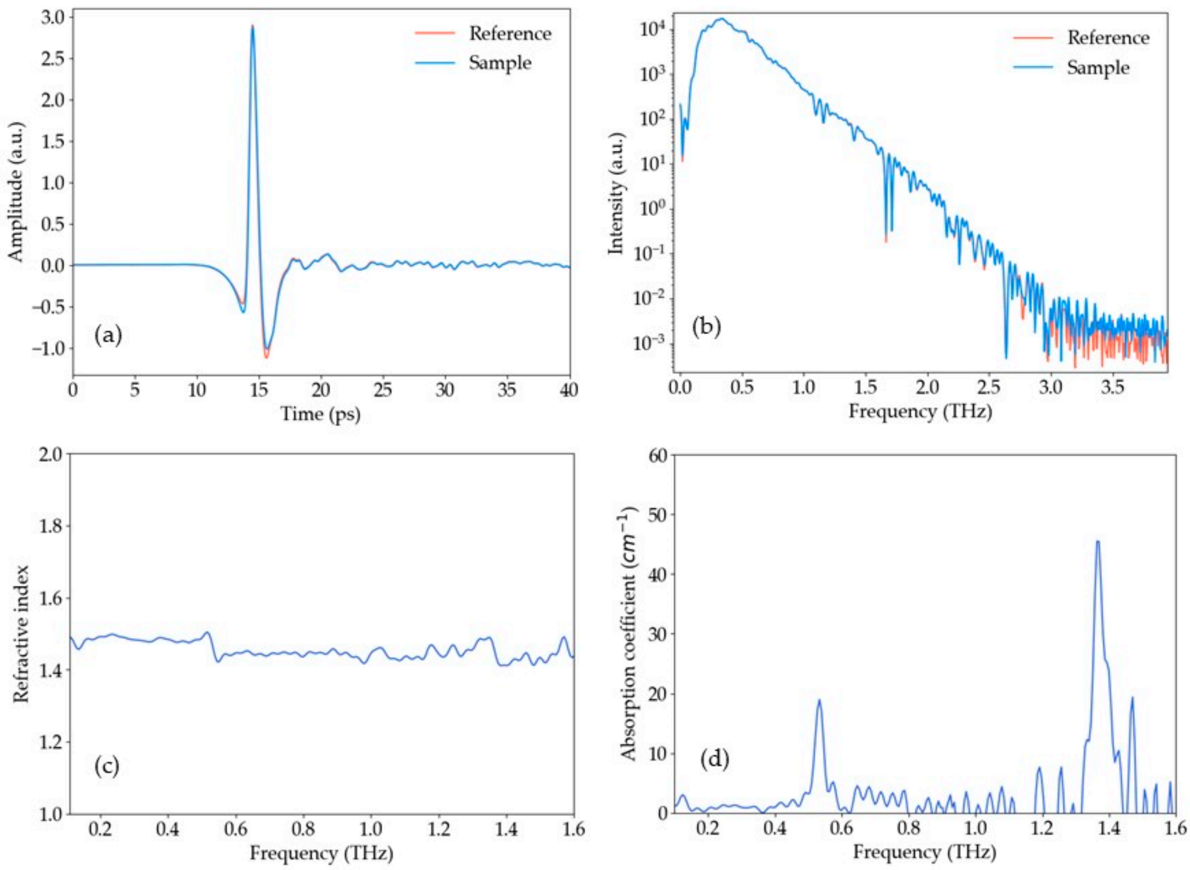

Figure 4. (**a**) The THz time domain reference and sample pulses, (**b**) their respective intensity spectra, (**c**) refractive index, (**d**) absorption coefficient of lactose sample.

The ratio of the sample signal to the reference signal is written as

$$\frac{E_{Sam}(\omega)}{E_{Ref}(\omega)} = R\exp(-i\Delta\varphi) \tag{2}$$

Here, $\Delta\varphi(\omega) = \varphi_{Sam}(\omega) - \varphi_{Ref}(\omega)$ is the phase difference and R is the amplitude reflectance written as

$$R(\omega) = \frac{|E_{Sam}(\omega)|}{\left|E_{Ref}(\omega)\right|} \tag{3}$$

Next, the complex refractive index $\tilde{n} = n + ik$ is computed as follows [31–33]:

$$\tilde{n}^2(\omega) = \frac{\sin^2\theta_i\cdot\left(1 - \sqrt{1 - 4\cdot(\sin\varphi_{sam}\cdot\cos\varphi_{sam})^2}\right)}{2\cdot(\sin\varphi_{sam}\cdot\cos\varphi_{sam})^2}{n_1}^2 \tag{4}$$

where,

$$\sin\varphi_{sam}\cdot\cos\varphi_{sam} = \frac{q\sin^2\theta_i\cos^2\theta_i + \sin\theta_i\cos\theta_i\sin\varphi_{ref}\cos\varphi_{ref}}{\sin\theta_i\cos\theta_i + q\sin\varphi_{ref}\cos\varphi_{ref}} \tag{5}$$

and

$$q = \frac{1 - R(\omega)\exp(-i\Delta\varphi)}{1 + R(\omega)\exp(-i\Delta\varphi)} \tag{6}$$

Finally, the absorption coefficient (α) is calculated as follows:

$$\alpha(\omega) = \frac{2\omega k(\omega)}{c} \tag{7}$$

Figure 4c,d shows the refractive index and absorption coefficient of the lactose sample. The unique absorption features of lactose at 0.53 THz and 1.39 THz are clearly visible. These absorption peaks are consistent with the previously reported values [20,21].

In the next step, we measured the refractive index and absorption coefficient of the lactose sample, which was packaged in a polyethylene bag as shown in Figure 3a. The sample was placed on the Si prism as shown in Figure 3b. The sample was pressed to avoid the air gap between the prism and the sample. The refractive index and absorption coefficient of the sample were computed using Equation (4) and are shown in Figure 5a,b, respectively.

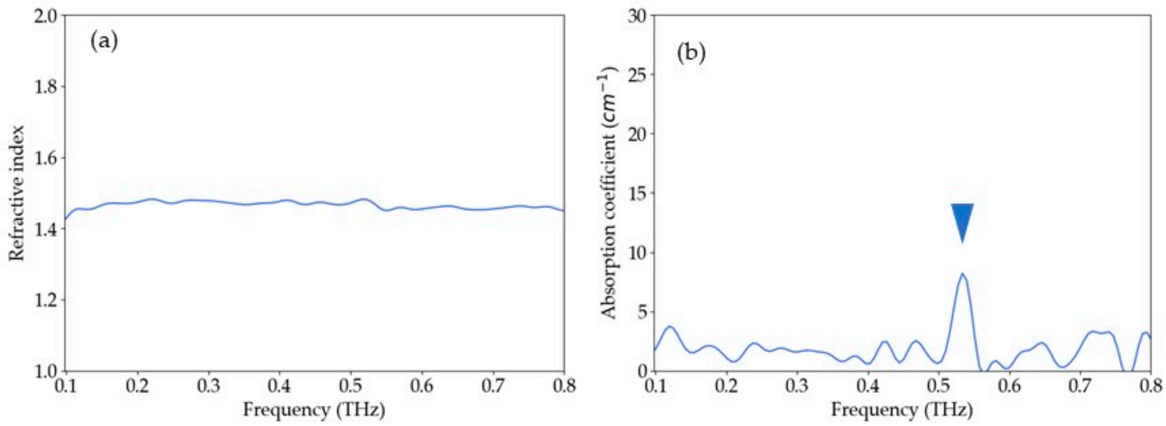

Figure 5. (**a**) The refractive index and (**b**) the absorption coefficient of the packaged sample. The absorption peak at 0.53 THz is clearly visible, as shown by the arrowhead. Since the penetration depth of the evanescent wave is smaller than the thickness of the plastic bag at high frequencies, the absorption features of the lactose sample at high frequency cannot be measured reliably. Therefore, the absorption coefficient is shown up to 0.8 THz.

Despite the fact that lactose has clear absorption peaks, as seen in Figure 4d, only the first absorption peak at 0.53 THz was identified when the sample was packaged in the polyethylene bag. At sub-THz frequencies, the penetration depth of the evanescent wave was in the range of few tens of micrometer, making it possible to identify the absorption peak at 0.53 THz. However, the penetration depth of evanescent wave decreased with the increase in frequency, as seen in Figure 2. Therefore, the absorption features of the lactose sample at high frequency cannot be measured reliably. The overall results indicate that the packaged samples with spectral fingerprints in a sub-terahertz frequency range can be identified using attenuated total reflection terahertz time domain spectroscopy [34]. However, terahertz properties of other packaging materials, such as papers and fabrics, need to be investigated to further expand the application of this system.

4. Conclusions

Non-destructive testing is one of the potential applications of terahertz waves. Several reports have been published showing that drugs and explosives in various covering materials, such as cardboard and fabrics, can be identified based upon their spectral fingerprint using transmission mode terahertz spectroscopy. However, samples with high terahertz absorption cannot be measured using such a system. Here, we demonstrated that the terahertz time domain attenuated total reflection spectroscopy can be used to non-destructively identify the samples packaged in a thin polyethylene bag based upon their spectral fingerprints. In the sub-terahertz frequency region, the penetration depth of the evanescent wave is larger than the thickness of typical plastic bag, allowing us to obtain the absorption features of the sample. We believe that this technique can be used to identify samples such as medicine sachets to prevent medication errors in pharmacies.

Author Contributions: All the measurements were done by K.H. The project was supervised by S.R.T. All authors have read and agreed to the published version of the manuscript.

Funding: Part of the research was supported by the JSPS Grant-in-Aid for Scientific Research C (21K04174).

Institutional Review Board Statement: Not applicable.

Informed Consent Statement: Not applicable.

Data Availability Statement: Not applicable.

Conflicts of Interest: The authors declare no conflict of interest.

References

1. Jepsen, P.U.; Cooke, D.G.; Koch, M. Terahertz Spectroscopy and Imaging—Modern Techniques and Applications. *Laser Photonics Rev.* **2010**, *5*, 124–166. [CrossRef]
2. Ferguson, B.; Zhang, X.-C. Materials for Terahertz Science and Technology. *Nat. Mater.* **2002**, *1*, 26–33. [CrossRef]
3. Kato, M.; Tripathi, S.R.; Murate, K.; Imayama, K.; Kawase, K. Non-Destructive Drug Inspection in Covering Materials Using a Terahertz Spectral Imaging System with Injection-Seeded Terahertz Parametric Generation and Detection. *Opt. Express* **2016**, *24*, 6425. [CrossRef]
4. Kawase, K.; Ogawa, Y.; Watanabe, Y.; Inoue, H. Non-Destructive Terahertz Imaging of Illicit Drugs Using Spectral Fingerprints. *Opt. Express* **2003**, *11*, 2549. [CrossRef]
5. Shen, Y.C.; Lo, T.; Taday, P.F.; Cole, B.E.; Tribe, W.R.; Kemp, M.C. Detection and Identification of Explosives Using Terahertz Pulsed Spectroscopic Imaging. *Appl. Phys. Lett.* **2005**, *86*, 241116. [CrossRef]
6. Neu, J.; Schmuttenmaer, C.A. Tutorial: An Introduction to Terahertz Time Domain Spectroscopy (THz-TDS). *J. Appl. Phys.* **2018**, *124*, 231101. [CrossRef]
7. Withayachumnankul, W.; Naftaly, M. Fundamentals of Measurement in Terahertz Time-Domain Spectroscopy. *J. Infrared Millim. Terahertz Waves* **2013**, *35*, 610–637. [CrossRef]
8. Tripathi, S.R.; Aoki, M.; Takeda, M.; Asahi, T.; Hosako, I.; Hiromoto, N. Accurate Complex Refractive Index with Standard Deviation of ZnTe Measured by Terahertz Time Domain Spectroscopy. *Jpn. J. Appl. Phys.* **2013**, *52*, 042401. [CrossRef]
9. Jordens, C. Detection of Foreign Bodies in Chocolate with Pulsed Terahertz Spectroscopy. *Opt. Eng.* **2008**, *47*, 037003. [CrossRef]
10. Ok, G.; Kim, H.J.; Chun, H.S.; Choi, S.-W. Foreign-Body Detection in Dry Food Using Continuous Sub-Terahertz Wave Imaging. *Food Control* **2014**, *42*, 284–289. [CrossRef]
11. Tripathi, S.R.; Ogura, H.; Kawagoe, H.; Inoue, H.; Hasegawa, T.; Takeya, K.; Kawase, K. Measurement of Chloride Ion Concentration in Concrete Structures Using Terahertz Time Domain Spectroscopy (THz-TDS). *Corros. Sci.* **2012**, *62*, 5–10. [CrossRef]
12. Reid, M.; Fedosejevs, R. Terahertz Birefringence and Attenuation Properties of Wood and Paper. *Appl. Opt.* **2006**, *45*, 2766. [CrossRef]
13. Saleh, B.E.A. *Fundamentals of Photonics*; Wiley: Hoboken, NJ, USA, 2019.
14. Withayachumnankul, W.; Fischer, B.M.; Lin, H.; Abbott, D. Uncertainty in Terahertz Time-Domain Spectroscopy Measurement. *J. Opt. Soc. Am. B* **2008**, *25*, 1059. [CrossRef]
15. Takagi, S.; Takahashi, S.; Takeya, K.; Tripathi, S.R. Influence of Delay Stage Positioning Error on Signal-To-Noise Ratio, Dynamic Range, and Bandwidth of Terahertz Time-Domain Spectroscopy. *Appl. Opt.* **2020**, *59*, 841. [CrossRef] [PubMed]
16. Nashima, S.; Morikawa, O.; Takata, K.; Hangyo, M. Measurement of Optical Properties of Highly Doped Silicon by Terahertz Time Domain Reflection Spectroscopy. *Appl. Phys. Lett.* **2001**, *79*, 3923–3925. [CrossRef]
17. Vilagosh, Z.; Lajevardipour, A.; Appadoo, D.; Juodkazis, S.; Wood, A.W. Using Attenuated Total Reflection (ATR) Apparatus to Investigate the Temperature Dependent Dielectric Properties of Water, Ice, and Tissue-Representative Fats. *Appl. Sci.* **2021**, *11*, 2544. [CrossRef]
18. Huang, Y.; Singh, R.; Xie, L.; Ying, Y. Attenuated Total Reflection for Terahertz Modulation, Sensing, Spectroscopy and Imaging Applications: A Review. *Appl. Sci.* **2020**, *10*, 4688. [CrossRef]
19. Ryu, M.; Ng, S.H.; Anand, V.; Lundgaard, S.; Hu, J.; Katkus, T.; Appadoo, D.; Vilagosh, Z.; Wood, A.W.; Juodkazis, S.; et al. Attenuated Total Reflection at THz Wavelengths: Prospective Use of Total Internal Reflection and Polariscopy. *Appl. Sci.* **2021**, *11*, 7632. [CrossRef]

20. Hirori, H.; Yamashita, K.; Nagai, M.; Tanaka, K. Attenuated Total Reflection Spectroscopy in Time Domain Using Terahertz Coherent Pulses. *Jpn. J. Appl. Phys.* **2004**, *43*, L1287–L1289. [CrossRef]
21. Tripathi, S.R.; Inoue, H.; Hasegawa, T.; Kawase, K. Non-Destructive Inspection of Chloride Ion in Concrete Structures Using Attenuated Total Reflection of Millimeter Waves. *J. Infrared Millim. Terahertz Waves* **2013**, *34*, 181–186. [CrossRef]
22. Nagai, M.; Yada, H.; Arikawa, T.; Tanaka, K. Terahertz Time-Domain Attenuated Total Reflection Spectroscopy in Water and Biological Solution. *Int. J. Infrared Millim. Waves* **2007**, *27*, 505–515. [CrossRef]
23. Mendoza-Galvan, A.; Mendez-Lara, J.G.; Mauricio-Sanchez, R.A.; Jarrendahl, K.; Arwin, H. Effective Absorption Coefficient and Effective Thickness in Attenuated Total Reflection Spectroscopy. *Opt. Lett.* **2021**, *46*, 872. [CrossRef] [PubMed]
24. Brown, E.R.; Bjarnason, J.E.; Fedor, A.M.; Korter, T.M. On the Strong and Narrow Absorption Signature in Lactose at 0.53 THz. *Appl. Phys. Lett.* **2007**, *90*, 061908. [CrossRef]
25. James, K.L.; Barlow, D.; McArtney, R.; Hiom, S.; Roberts, D.; Whittlesea, C. Incidence, Type and Causes of Dispensing Errors: A Review of the Literature. *Int. J. Pharm. Pract.* **2009**, *17*, 9–30. [CrossRef]
26. Poon, E.G.; Cina, J.L.; Churchill, W.; Patel, N.; Featherstone, E.; Rothschild, J.M.; Keohane, C.A.; Whittemore, A.D.; Bates, D.W.; Gandhi, T.K. Medication Dispensing Errors and Potential Adverse Drug Events before and after Implementing Bar Code Technology in the Pharmacy. *Ann. Intern. Med.* **2006**, *145*, 426. [CrossRef] [PubMed]
27. Dai, J.; Zhang, J.; Zhang, W.; Grischkowsky, D. Terahertz Time-Domain Spectroscopy Characterization of the Far-Infrared Absorption and Index of Refraction of High-Resistivity, Float-Zone Silicon. *J. Opt. Soc. Am. B* **2004**, *21*, 1379. [CrossRef]
28. Hecht, E. *Optics. Hecht*; Addison-Wesley: Reading, MA, USA, 1998.
29. Kaushik, M.; Ng, B.W.-H.; Fischer, B.M.; Abbott, D. Reduction of Scattering Effects in THz-TDS Signals. *IEEE Photonics Technol. Lett.* **2012**, *24*, 155–157. [CrossRef]
30. Jin, Y.S.; Kim, G.J.; Jeon, S.G. Terahertz Dielectric Properties of Polymers. *J. Korean Phys. Soc.* **2006**, *49*, 513–517.
31. Nakanishi, A.; Kawada, Y.; Yasuda, T.; Akiyama, K.; Takahashi, H. Terahertz Time Domain Attenuated Total Reflection Spectroscopy with an Integrated Prism System. *Rev. Sci. Instrum.* **2012**, *83*, 033103. [CrossRef]
32. Soltani, A.; Jahn, D.; Duschek, L.; Castro-Camus, E.; Koch, M.; Withayachumnankul, W. Attenuated Total Reflection Terahertz Time-Domain Spectroscopy: Uncertainty Analysis and Reduction Scheme. *IEEE Trans. Terahertz Sci. Technol.* **2016**, *6*, 32–39. [CrossRef]
33. Soltani, A.; Probst, T.; Busch, S.F.; Schwerdtfeger, M.; Castro-Camus, E.; Koch, M. Error from Delay Drift in Terahertz Attenuated Total Reflection Spectroscopy. *J. Infrared Millim. Terahertz Waves* **2014**, *35*, 468–477. [CrossRef]
34. Davies, A.G.; Burnett, A.D.; Fan, W.; Linfield, E.H.; Cunningham, J.E. Terahertz Spectroscopy of Explosives and Drugs. *Mater. Today* **2008**, *11*, 18–26. [CrossRef]